

# Comparison of *TP53* mutations in myelodysplasia and acute leukemia suggests divergent roles in initiation and progression

Ashwini Jambhekar,<sup>1,2</sup> Emily E. Ackerman,<sup>1</sup> Berk A. Alpay,<sup>3,4</sup> Galit Lahav,<sup>1,2</sup> and Scott B. Lovitch<sup>5</sup>

<sup>1</sup>Department of Systems Biology, Harvard Medical School, Boston, MA; <sup>2</sup>Ludwig Center at Harvard, Boston, MA; <sup>3</sup>Systems, Synthetic, and Quantitative Biology Program and

<sup>4</sup>Department of Organismal and Evolutionary Biology, Harvard University, Cambridge, MA; and <sup>5</sup>Department of Pathology, Brigham and Women's Hospital, Boston, MA

## Key Points

- *TP53* mutations in myelodysplastic syndrome and acute myeloid leukemia differ significantly in distribution and functional consequences.
- These differences suggest distinct biological roles for mutated p53 in initiation of myeloid dysplasia and progression to acute leukemia.

*TP53* mutation predicts adverse prognosis in many cancers, including myeloid neoplasms, but the mechanisms by which specific mutations affect disease biology, and whether they differ between disease categories, remain unknown. We analyzed *TP53* mutations in 4 myeloid neoplasm subtypes (myelodysplastic syndrome [MDS], acute myeloid leukemia [AML], AML with myelodysplasia-related changes [AML-MRC], and therapy-related AML), and identified differences in mutation types, spectrum, and hot spots between disease categories and in comparison to solid tumors. Missense mutations in the DNA-binding domain were most common across all categories, whereas inactivating mutations and mutations outside the DNA binding domain were more common in AML-MRC than in MDS. *TP53* mutations in MDS were more likely to retain transcriptional activity, and comutation profiles were distinct between disease categories and mutation types. Our findings suggest that mutated *TP53* contributes to initiation and progression of neoplasia via distinct mechanisms, and support the utility of specific identification of *TP53* mutations in myeloid malignancies.

## Introduction

The transcription factor p53, encoded by the *TP53* gene, functions as a tumor suppressor in multiple tissues.<sup>1</sup> *TP53* is the most frequently mutated gene in human cancers, with mutation incidence exceeding 50% for many cancer types.<sup>2</sup> In myeloid neoplasms, *TP53* mutations occur in ~10% of cases,<sup>3,4</sup> and, as for solid tumors, are strong and independent predictors of adverse prognosis, including failure of induction chemotherapy, relapse after hematopoietic stem cell transplantation, and reduced overall survival.<sup>5-8</sup>

Myeloid neoplasms have traditionally been divided into myelodysplastic syndromes (MDS) and acute myeloid leukemia (AML) by blast enumeration, with >20% blasts in the blood or bone marrow generally required for classification as AML; this division persists in the current World Health Organization (WHO) classification<sup>9</sup> and International Consensus Classification (ICC).<sup>10</sup> AML arising via progression from MDS, or after cytotoxic chemotherapy or radiation, have worse prognosis than de novo AML and are separately classified; these categories were defined as AML with myelodysplasia-related changes

Submitted 19 October 2023; accepted 8 February 2024; prepublished online 15 February 2024; final version published online 12 March 2024. <https://doi.org/10.1016/j.bneo.2024.100004>.

Presented, in part, as a selected oral abstract at the United States and Canadian Academy of Pathology annual meeting, New Orleans, LA, 14 March 2023.

Data are available on request from the corresponding author, Scott B. Lovitch ([slovitch@bwh.harvard.edu](mailto:slovitch@bwh.harvard.edu)).

The online version of this article contains a data supplement.

© 2024 by The American Society of Hematology. Licensed under [Creative Commons Attribution-NonCommercial-NoDerivatives 4.0 International \(CC BY-NC-ND 4.0\)](#), permitting only noncommercial, nonderivative use with attribution. All other rights reserved.

(AML-MRC) and therapy-related AML (t-AML) in the revised fourth edition WHO classification, and are maintained in the fifth edition WHO classification and ICC.

The studies of Valk et al<sup>11</sup> and Weinberg et al<sup>12</sup> demonstrated that the prognostic impact of *TP53* mutation cuts across these traditional classifications, with *TP53*-mutated MDS and AML showing similarly poor prognosis; consequently, the WHO fifth edition and ICC both recognize *TP53*-mutated myeloid neoplasia as a specific disease category.<sup>9,10</sup> Subsequent studies have filled in important details about the relationship between *TP53* mutation and clinical outcomes in MDS and AML, including the role of variant allele fraction (VAF) and the impact of multiple “hits” to *TP53*. It is now well established that increased VAF of the *TP53* mutation correlates with worse outcomes.<sup>13</sup> The relationship between presence of single vs multiple hits to *TP53* and prognosis appears more complex; initial studies reported adverse outcomes only with multiple hits to *TP53*,<sup>14</sup> but subsequent studies demonstrated dismal outcomes even with monoallelic *TP53* mutation.<sup>12,15</sup> Recent studies have suggested that this distinction may vary by classification (ie, AML vs MDS),<sup>16</sup> and based on blast count and genomic landscape.<sup>17</sup>

By contrast, the impact of specific *TP53* mutations and mutation types has not been adequately studied. *TP53* is unusual among tumor suppressor genes in that mutations are strongly biased toward missense mutations, which potentially retain function, rather than inactivating mutations, and these mutations are enriched in the DNA-binding domain (DBD), with ~30% of mutations occurring at 7 “hot spots,” all within the DBD.<sup>18</sup> The vast majority of missense mutations compromise its transcriptional activity, resulting in accumulation of mutant p53 because of its failure to induce MDM2, the E3 ubiquitin ligase that mediates its degradation. However, p53 missense mutations can retain some transcriptional activity: analysis of 2314 p53 mutants in a reporter assay revealed transcriptional activities from none to wild-type (WT) levels, with most DBD mutations reducing activity below 20% of that of WT p53.<sup>19</sup> These properties raise the possibility that different *TP53* mutation classes (eg, missense vs truncating), or even specific mutations, may drive neoplasia by distinct mechanisms and differentially affect prognosis. In support of this, a recent study demonstrated that the distribution of p53 mutational hot spots varies between AML subtypes, suggesting that there may be distinct and context-dependent roles for different mutations.<sup>20</sup> However, there has not been any comprehensive assessment of the distribution of p53 mutations across broader categories of myeloid neoplasia, for example, MDS vs AML, or between hematologic neoplasms and solid tumors; neither WHO fifth edition nor ICC criteria distinguishes between *TP53* mutation types. Given accumulating data indicating that *TP53* mutational status informs optimal therapy in addition to prognosis,<sup>21-23</sup> and development of novel therapies directly targeting mutant p53 protein,<sup>24-27</sup> it is critical to understand the nature of p53 mutations in these diseases, and their biological functions in modulating disease initiation or progression.

In this study, we analyzed *TP53* mutations in myeloid neoplasms, comparing relative frequencies of mutation types, distributions across the p53 protein, and functional consequences between myeloid neoplasms and solid tumors and across categories of myeloid neoplasia. We identified significant differences between disease categories in types and locations of mutations, transcriptional capacity, and comutation profiles, with the greatest

differences occurring between MDS and AML-MRC. These results suggest that *TP53* mutations may play distinct pathogenic roles in different categories of myeloid disease, and that different functional categories of *TP53* mutation may mediate initiation and progression of myeloid neoplasia.

## Methods

### Study cohort

We identified *TP53* mutant cases of AML, MDS, AML-MRC, and t-AML in the cBioPortal database, a public-facing repository that incorporates data from multiple studies,<sup>28,29</sup> and in the Hematologic Malignancies Data Repository of the Dana-Farber Cancer Institute. From cBioPortal, we incorporated AML data sets from Oregon Health and Science University<sup>30</sup> and the Cancer Genome Atlas<sup>3</sup>; MDS data sets from the University of Tokyo<sup>31</sup> and Memorial Sloan-Kettering Cancer Center (MSKCC)<sup>30,32</sup>; and an MDS/AML data set from Washington University in St. Louis.<sup>33</sup> All cases in both data sets were annotated with diagnostic classification and mutation(s) identified by next-generation sequencing, including nucleotide change, amino acid change, and VAF; additional information, including karyotype, treatment history, and clinical outcome, was available for a limited subset of cases. The data sets were not significantly different in terms of the ratios of missense to inactivating *TP53* mutations within disease categories. The only exception was the Vanderbilt-Ingram Cancer Center (VICC) data set, which had fewer missense mutations in all disease categories but otherwise reflected the same trends seen in the other data sets. Duplicates within and between databases were manually filtered and removed, and only cases with *TP53* mutations annotated as pathogenic or likely pathogenic were included in the analysis (ie, nonpathogenic variants were excluded). After filtering, there were a total of 1117 independent instances of *TP53* mutations in myeloid neoplasms, representing 536, 349, 167, and 65 instances in AML, MDS, AML-MRC, and t-AML, respectively. We classified *TP53* mutations as nonsense, frameshift, splice, in-frame indel, or missense, and calculated the frequency of each mutation type in each disease. Information on large deletions was not available. When samples from the same patient were sequenced multiple times, replicates were removed for cataloging p53 mutations but were retained for analyses involving VAF and comutations to capture evolving changes. For survival analysis of individuals with multiple *TP53* mutations, the mutation with the highest VAF was considered.

### Peak finding

Peaks in mutation frequency above background were identified by find\_peaks from SciPy's Signal processing in Python 3.8.

### Comutation analysis

Data were obtained from cBioPortal using the cBioPortalData Bioconductor package in R version 4.1.3 from the previously identified studies. All comutation plots were created using the CoMut python package.

### Statistical analyses

Continuous variables were compared by Welch *t* test. Categorical variables were compared pair-wise by Fisher exact test. Fisher

exact test was also used for comutation studies. In all cases, Bonferroni corrections for multiple hypothesis tests were applied.

Comparison of underlying mutation frequencies across disease categories

Using the data set of missense mutations in AML, MDS, and AML-MRC, letting  $d$  denote the disease and  $l$  the number of codons, we observed a vector of integers  $y_d = (y_{d1}, y_{d2}, \dots, y_{dl})$  for each disease. In total, 411 mutations were observed among patients with AML, 286 for those with MDS, and 113 for those with AML-MRC. Considering only codons with at least 1 mutation recorded under any disease, we have that  $l = 121$ . Assuming  $y_d \sim \text{Multinomial}(\sum y_d, \theta_d)$  and  $\theta_d \stackrel{iid}{\sim} \text{Dirichlet}(\alpha)$ , then  $\theta_d | y_d \sim \text{Dirichlet}(\alpha + y_d)$ . We set  $\alpha$  such that  $\alpha_i = \sum_d y_{di}$ , as an empirical prior. We compared myeloid neoplasms with the Institute for Systems Biology Cancer Genomics Cloud (ISB-CGC) data set using a similar framework but with different priors and  $l = 378$ . Specifically, we set  $\theta_{\text{ISB}} \sim \text{Dirichlet}$ -distributed with concentration parameter 0.1, and  $\theta_{\text{MN}} \sim \text{Dirichlet}(y_{\text{ISB}} / \sum y_{\text{ISB}} \times 35)$ . Code used for sampling can be found at <https://github.com/berkalpay/tp53mutations/>.

Transcriptional activity analysis

Transcriptional activity scores were obtained from the PHANTM database (<http://mutantp53.broadinstitute.org>), which draws its data from the study of Kato et al.<sup>19</sup>

Results

TP53 mutation types and locations vary between myeloid neoplasms

In the analyzed data sets, 6.9% to 23.5% myeloid neoplasia cases were TP53 mutant, consistent with previously reported statistics.<sup>3</sup> In total, the analyzed data sets included 414 unique mutations; ~20% of samples contained multiple TP53 mutations, with <3% containing ≥3 mutations (Table 1). The distribution of VAFs was similar between disease categories except for MDS, which had significantly lower VAFs, consistent with expected lower blast counts (supplemental Figure 1A; supplemental Table 1). Patterns of single-nucleotide substitutions in TP53 were similar between diseases; C→T mutations, which showed a coding strand bias, comprised approximately half of all single-nucleotide changes, consistent with mutations arising from DNA methylation (supplemental Figure 1B). In samples with multiple mutations, VAFs

were generally within a twofold range, indicating that the mutations arose at similar points in disease progression (supplemental Figure 1C, region between gray lines).

Missense mutations were most prevalent across all disease categories, as expected.<sup>20,34,35</sup> Nevertheless, the spectrum of mutation types varied between neoplasms, with MDS showing significantly more missense mutations and fewer splice-site mutations than AML-MRC (Figure 1A; supplemental Figure 1D). This trend was maintained among cases with multiple TP53 mutations (Figure 1B) or with VAF of ≥0.55, a proxy for loss of heterozygosity (Figure 1C). We did not observe significant differences in mutation spectrum between cases with and without complex karyotype; however, only a subset of cases in the data set contained full karyotype information, limiting the statistical power of our analysis. Because the data sets pooled multiple studies, resulting in heterogeneous patient populations, we repeated this analysis on 2 individual studies, the MSKCC (2020) cohort and the VICC cohort. In both cases, results were similar to those observed with the parent (pooled) data set, with missense mutations enriched and splice mutations depleted in MDS compared with AML-MRC (supplemental Figure 1E-F). Notably, these results narrowly failed to achieve significance in the Memorial Sloan-Kettering data set, demonstrating the importance of analyzing the larger, pooled data sets to obtain sufficient sample sizes to achieve statistical significance while retaining the overall trends of individual studies.

Although mutations were strongly enriched in the DBD for all disease categories, as reported,<sup>20</sup> DBD enrichment was significantly higher in MDS than in AML or AML-MRC (Figure 1D). A nuclear localization sequence-containing region adjacent to the DBD was significantly enriched for mutations in AML-MRC (Figure 1D). In all disease categories, >80% of DBD mutations were missense, consistent with reports in other cancer types (t-AML was omitted from this and subsequent analyses, because of its small sample size).<sup>34,35</sup> By contrast, frameshift and nonsense mutations occurred relatively more frequently in other regions, particularly in the nuclear localization sequence (Figure 1E). The first activation domain did not contain any nonsense mutations in any disease category (Figure 1C). Overall, these results recapitulated the general trend of enrichment of missense mutations in the TP53 DBD,<sup>34,35</sup> and reveal differences in mutation type and location between myeloid neoplasms, including relative enrichment of null and splice-site mutations in AML-MRC compared with MDS.

Analysis of distribution of TP53 mutations reveals myeloid-specific and disease-specific hot spots

To obtain a more granular view of the types and locations of TP53 mutations, we constructed lollipop plots depicting the frequency of missense, nonsense, and frameshift mutations at each codon in each disease (Figure 2A). Of 393 amino acids, 195 were mutated at least once; 128 mutated positions harbored missense mutations, and 27 positions showed examples of both missense and null mutations, with a general bias toward missense mutations. To determine whether the overall pattern of mutations (their locations and frequencies) differed between neoplasms, we plotted the cumulative fraction of all mutations along the length of the protein (Figure 2B). The greatest differences in the cumulative curves were seen between MDS and AML-MRC, with AML-MRC being biased toward C-terminal mutations (Figure 2B, lower). To identify

Table 1. Percentage of cases harboring the indicated number of distinct TP53 mutations

	Number of TP53 mutations		
	1, % (n)	2, % (n)	≥3, % (n)
AML	78.6 (338)	19.1 (82)	2.3 (10)
MDS	77.3 (214)	20.6 (57)	2.2 (6)
AML-MRC	79.5 (109)	19.0 (26)	1.5 (2)
t-AML	81.8 (45)	18.2 (10)	0 (0)

Cases were stratified by disease type, and the percentage of cases with 1, 2, and ≥3 mutations was determined. For patients of whom multiple samples were sequenced, the largest number of distinct TP53 mutations identified in a single sample was considered.

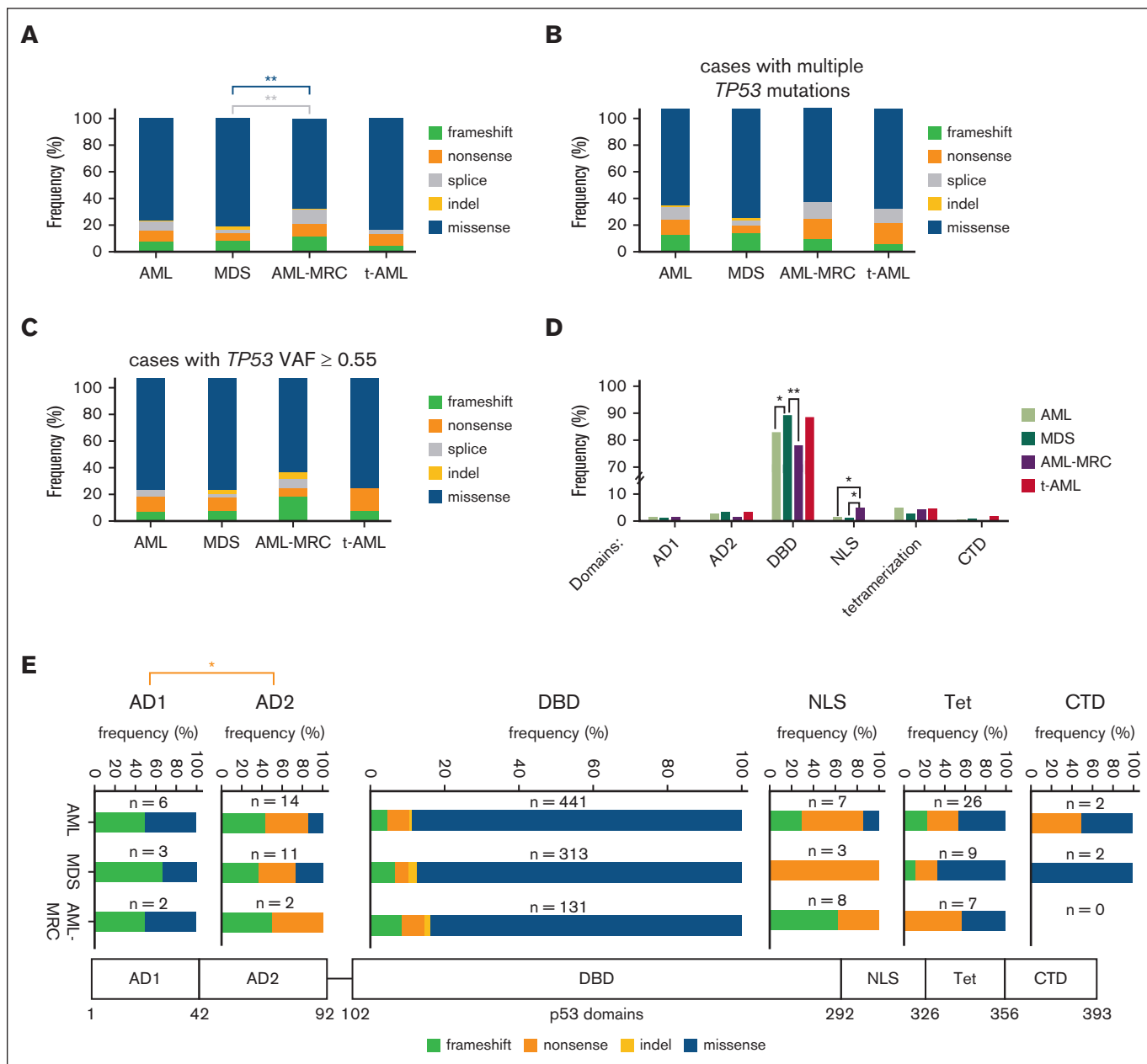


**Figure 1. *TP53* mutation types and locations differ between myeloid neoplasms.** (A) Frequency of frameshift, nonsense, indel, splice, and missense *TP53* mutations shown as a percentage of total *TP53* mutations in the indicated disease categories. (B) Frequency of each mutation type in cases with  $\geq 2$  *TP53* mutations in the indicated neoplasms (number of mutations: AML,  $n = 129$ ; MDS,  $n = 107$ ; AML-MRC,  $n = 40$ ; and t-AML,  $n = 14$ ). (C) Frequency of each mutation type in cases with mutant VAF of  $\geq 0.55$  in the indicated diseases. AML,  $n = 103$ ; MDS,  $n = 41$ ; AML-MRC,  $n = 47$ ; and t-AML,  $n = 13$ . (D) Frequency of mutations in each p53 domain shown as percentage of total number of mutations in each disease category. For panels A,D, AML,  $n = 536$ ; MDS,  $n = 349$ ; AML-MRC,  $n = 167$ ; and t-AML,  $n = 65$ . (E) Frequency of each mutation type by domain in AML, MDS, and AML-MRC. Domain boundaries are indicated. For adjacent domains, the C-terminal end of the boundary is shown. The total number of mutations in each domain is shown for each disease. Splice mutations are not shown. \* $P < .05$  and \*\* $P < .01$  by Fisher exact test with Bonferroni correction.

individual hot spot mutations in a quantitative and unbiased manner, we applied an algorithm that detects peaks in mutation frequency above local background levels. This analysis was conducted only for missense mutations because of the relative paucity of other mutation types. Of the 7 most common *TP53* mutation sites in human cancers<sup>18</sup> (subsequently referred to as “pan-cancer hot spots”), 6 were identified as peaks in AML (R175, Y220, G245,

R248, R273, and R282); R249 was the only hot spot in the pan-cancer set not identified as such in myeloid neoplasms (Figure 2C). MDS and AML-MRC additionally lacked hot spots at G245 and R282. Hot spot mutations have been classified as “contact” or “conformational” mutations based on their effects on DNA binding or protein folding, respectively.<sup>36</sup> Contact mutations (R248Q, R273H, and R282W) were more common in AML-MRC

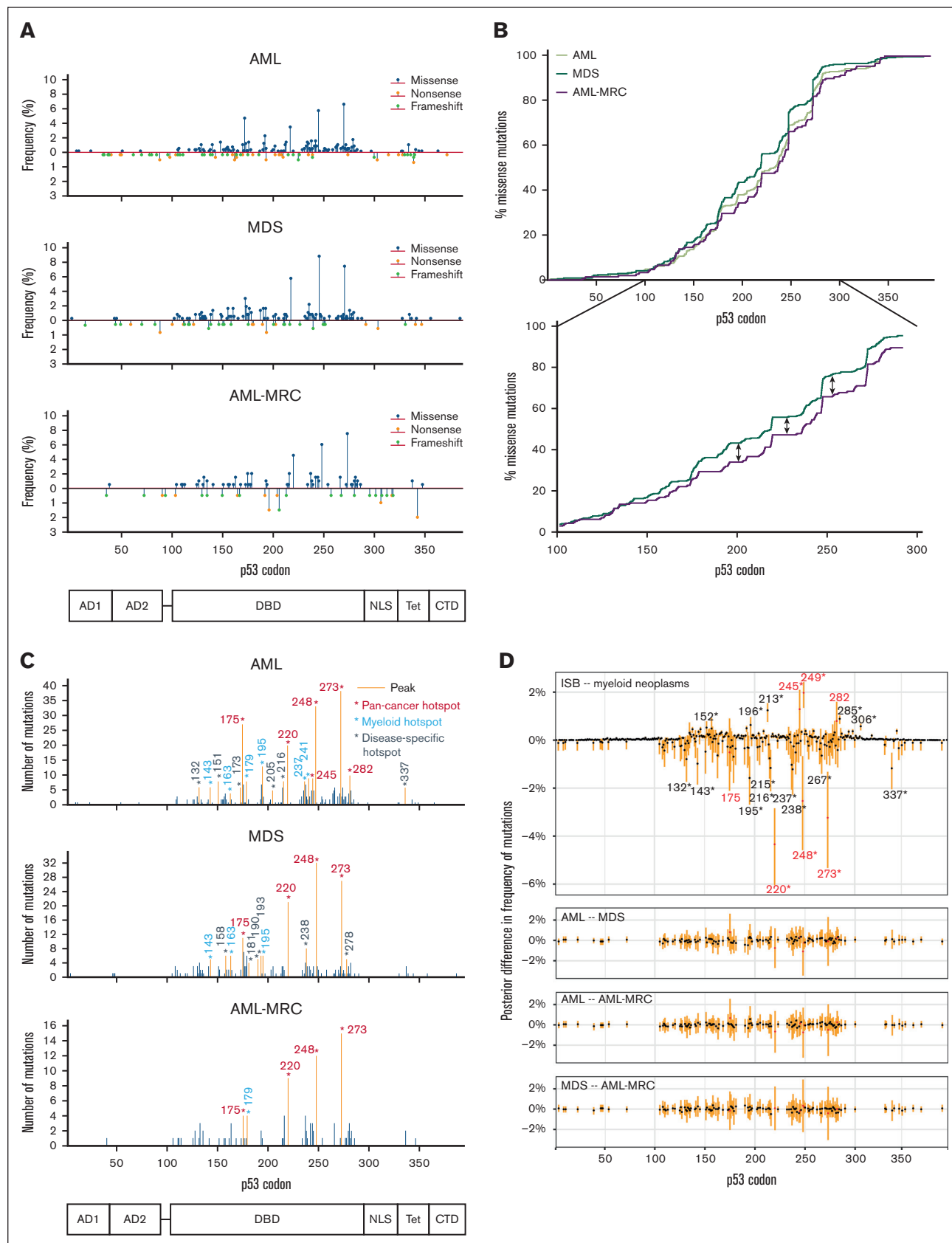


Figure 2.



(16.8%) than in either AML or MDS (10.9% and 12.9%, respectively), whereas conformational mutations (R175H, Y220C, G245S, and R249S) occurred with nearly equal prevalence in all categories (11.4%-12.4%). In addition to the 7 pan-cancer hot spots, we identified several hot spots in 2 of 3 diseases, which we termed “myeloid specific” (irrespective of their mutation rates in individual solid tumors). “Disease-specific” hot spots were defined as being present in only 1 disease. These results highlight the overall similarities in mutation patterns between myeloid neoplasms while also revealing differences in mutation distributions (frequency and location).

Next, we performed a Bayesian analysis to determine to what degree codons with missense mutations differed in their underlying mutation frequency between diseases. This analysis was performed for the pooled data set of myeloid neoplasms compared with the Institute for Systems Biology Cancer Genomics Cloud (ISB-CGC) data set of mutations derived from all cancer types to assess differences between hematologic malignancies and solid tumors.<sup>37</sup> It was separately conducted pair-wise for the different categories of myeloid neoplasms (Figure 2D). Sampling from the distributions of inferred mutation frequencies and then calculating the difference between them yielded a simulated expected difference with a 95% Bayesian credible interval for each codon. The largest expected difference between myeloid neoplasms and the pan-cancer data set was observed for mutations at codon Y220, which were enriched in myeloid neoplasms; mutations at R175, R248, and R273 were also over-represented in myeloid neoplasms, whereas mutations at R245, R249, and R282 were underrepresented. (Figure 2D, top panel). The estimated differences between the categories of myeloid neoplasms were smaller than those between myeloid neoplasms and solid tumors, with no individual codons at which the 95% Bayesian credible interval of the difference in mutation frequency excluded 0 occurring in any of the pair-wise comparisons (Figure 2D, bottom).

We then cataloged the amino acid changes resulting from missense mutations in each disease. Overall, 77 codons showed at least 2 different substitutions (Figure 3; supplemental Figure 2). C176 had the greatest diversity of substitutions, with mutations to F, G, R, S, W, and Y detected across diseases. The frequencies of specific substitutions varied between diseases at some positions. R273H was more prevalent in AML-MRC than in AML (9.5% vs 5.8%), with MDS showing an intermediate prevalence (7.3%; Figure 3). R248 was biased toward substitution to Q over W in MDS, whereas AML-MRC showed the opposite trend, and AML showed almost no bias. These patterns suggest both flexibility and specificity in pathogenic *TP53* mutations.

Overall, our findings demonstrate a distinct distribution of p53 mutations in myeloid neoplasms compared with solid tumors, and suggest distinct mutational patterns between individual myeloid neoplasms. The differences in amino acid substitutions between diseases at particular codons suggest distinct functional roles for specific p53 mutations in disease initiation and progression.

## Transcriptional activity and comutation profiles of *TP53* mutations differs between categories of myeloid neoplasia

To assess whether the biological consequences of mutated p53 might vary between types of myeloid neoplasia, we first calculated the distribution of transcriptional activity scores for missense mutations in each neoplasm<sup>19</sup> (see “Methods”), and found that it was significantly higher in MDS than in AML-MRC, with AML falling between these (Figure 4A). This result held true when the analysis was performed only on the subset of cases with VAF of  $\geq 0.55$ , indicating that it was not an artifact of the status of the second allele (Figure 4B).

To gain further insight into the interactions of mutant *TP53* with other oncogenic pathways, we investigated patterns of comutation between *TP53* and known leukemic driver genes. *DNMT3A*, *TET2*, and *NRAS* were commonly comutated with *TP53*, whereas *FLT3* and *NPM1* comutations were significantly less common than in cases with WT *TP53*, consistent with previous studies.<sup>20,38,39</sup> *FLT3* and *NPM1* mutations were underrepresented in *TP53*-mutant AMLs compared with *TP53*-WT AML (supplemental Figure 3; supplemental Table 3). When parsed by *TP53* mutation type, comutations in 26 driver genes were underrepresented in *TP53* nonsense and splice mutations (Figure 4C; supplemental Table 4): across samples with both single and multiple *TP53* mutations, the average number of comutations was 0.36 and 0.59 per *TP53* nonsense or splice mutation, respectively, compared with a comutation rate of 0.88 for *TP53* missense mutations. In AML-MRC, nonsense *TP53* mutations were significantly associated with comutation of *DNMT3A* (Figure 4D), with 2 of 6 *DNMT3A* mutations occurring with nonsense *TP53* (for comparison, none of the 19 *DNMT3A* mutations in MDS cooccurred with nonsense *TP53*). These findings provide further evidence that *TP53* null and splice-site mutations may mediate pathogenesis of myeloid neoplasms through distinct mechanisms from those of the more common missense mutations.

## Analysis of impact of *TP53* mutation class on outcomes in AML and AML-MRC

To investigate whether *TP53* mutation types affect patient outcomes, we first grouped *TP53* mutations as missense or null, with

**Figure 2. *TP53* mutational hot spots in myeloid neoplasms overlap with solid tumors but also include myeloid- and disease-specific peaks.** (A) Lollipop plot showing the frequency of missense (above axis) and nonsense and frameshift mutations (below axis) in the indicated disease categories. Frequency is shown as a percentage of total *TP53* mutations in each disease category; AML, n = 496; MDS, n = 331; and AML-MRC, n = 147. (B) Cumulative curve depicting the fraction of *TP53* missense mutations as a function of position (codon number) within the protein. Inset shows the cumulative curve in the DBD region for MDS and AML-MRC. Arrows show examples of regions in which the AML-MRC curve lags the MDS curve. (C) Identification of missense hot spots in the indicated diseases by peak-finding algorithm. Orange lines represent peaks identified by the algorithm, blue lines represent mutation sites not identified as peaks. Hot spots are classified as pan-cancer (from Leroy et al<sup>18</sup>), myeloid specific (occurring in  $\geq 2$  myeloid categories in this data set), or disease specific (unique in this data set). (D) Differences in underlying mutation frequency between the indicated disease categories at *TP53* codons with missense mutations were inferred using data from Figure 1A. Black points represent the expected value, and orange lines represent the central 95% Bayesian credible interval. Codons with no recorded mutations in the compared disease groups (Institute for Systems Biology pan-cancer dataset and myeloid neoplasms; and AML, MDS, and AML-MRC) were not considered. The expected difference in underlying mutation frequencies of pan-cancer hot spot codons are colored red. For panels B-D, AML, n = 411; MDS, n = 284; and AML-MRC, n = 113.

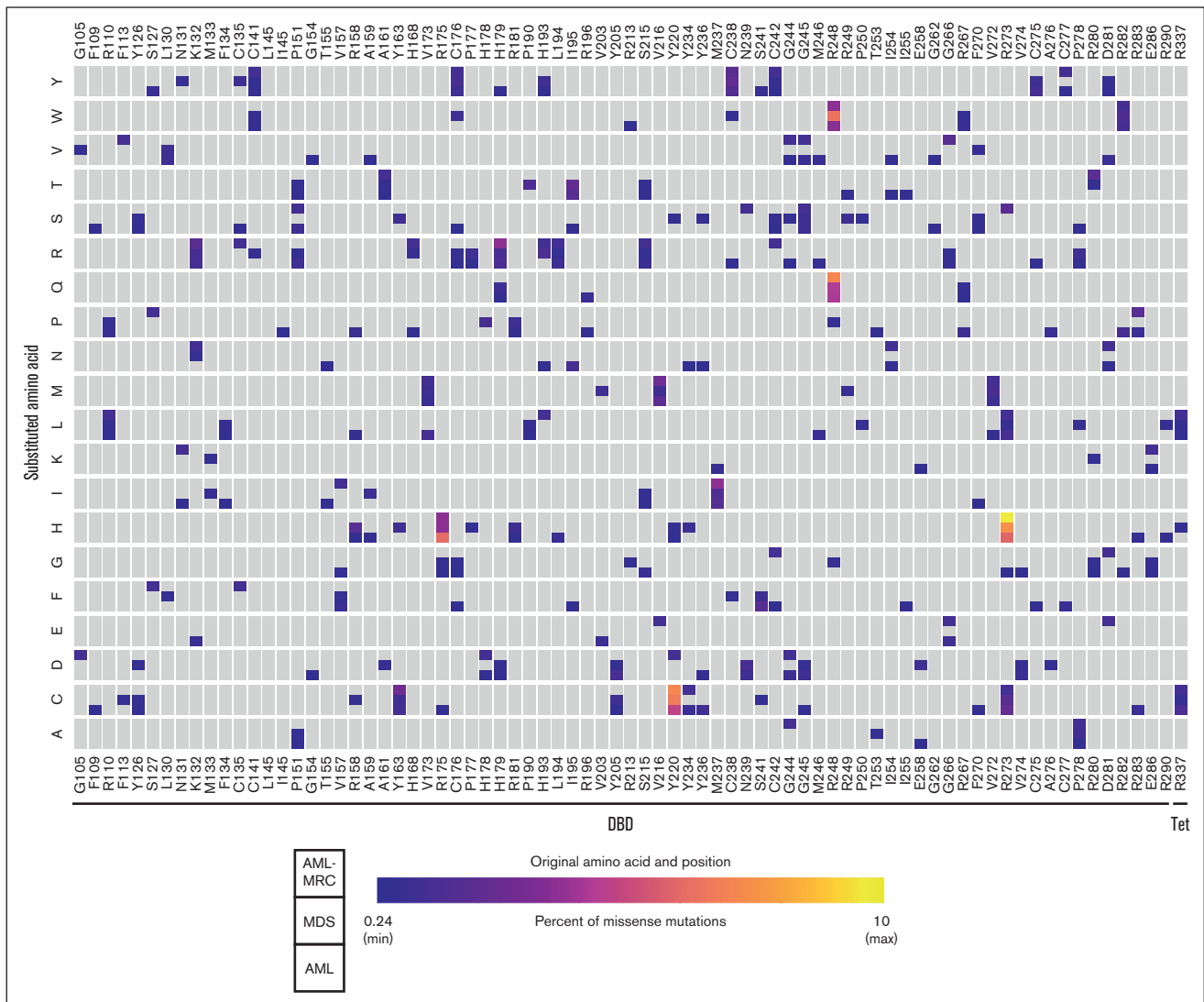


**Figure 3. *TP53* missense mutations show a wide diversity and disease-specific biases in amino acid substitutions.** Heat map depicting the frequency of each type of amino acid substitution at each codon. Only codons displaying multiple types of substitutions are shown. Each cell depicts the frequency of substitution in each of the 3 disease categories as depicted in the key. Gray boxes indicate no substitutions detected. The left end of the color spectrum represents 1 mutation event in the largest data set (AML; AML, n = 411; MDS, n = 284; and AML-MRC, n = 113).

the latter category comprised of frameshift, nonsense, and splice mutations. This grouping was chosen because of the distinct effects of the mutation type on p53 protein: null type mutations do not express detectable protein, whereas missense mutants tend to overexpress it. We observed a modest trend toward longer survival for p53-null cases in both AML and AML-MRC (Figure 4E-F), although survival for both null and missense mutations was shorter than that reported for WT p53.<sup>11,12</sup> These differences did not achieve statistical significance, and the small sample sizes involved and potential for confounding variables (eg, differences in treatment among patients at different institutions) precludes drawing definitive conclusions. However, these results suggest that *TP53* missense mutations may exert oncogenic effects in AML and AML-MRC beyond simply inactivating its tumor-suppressive function.

## Discussion

In this study, we identified differences in *TP53* mutations between myeloid neoplasms and solid tumors, as well as between subtypes of myeloid neoplasms, particularly between MDS and AML-MRC. These findings suggest discrete biological mechanisms for mutant p53 in hematologic malignancies, particularly in driving initiation and progression of myeloid neoplasia, and indicate that molecular and functional characterization of *TP53* mutations, as opposed to p53 immunohistochemistry alone, may be required for optimal assessment of *TP53*-mutant myeloid neoplasms in clinical practice. Notably, our analyses took advantage of large consortia that pool data from multiple independent studies and institutions (eg, cBioPortal) to uncover associations between *TP53* mutation types, functions, and disease categories. This approach has been

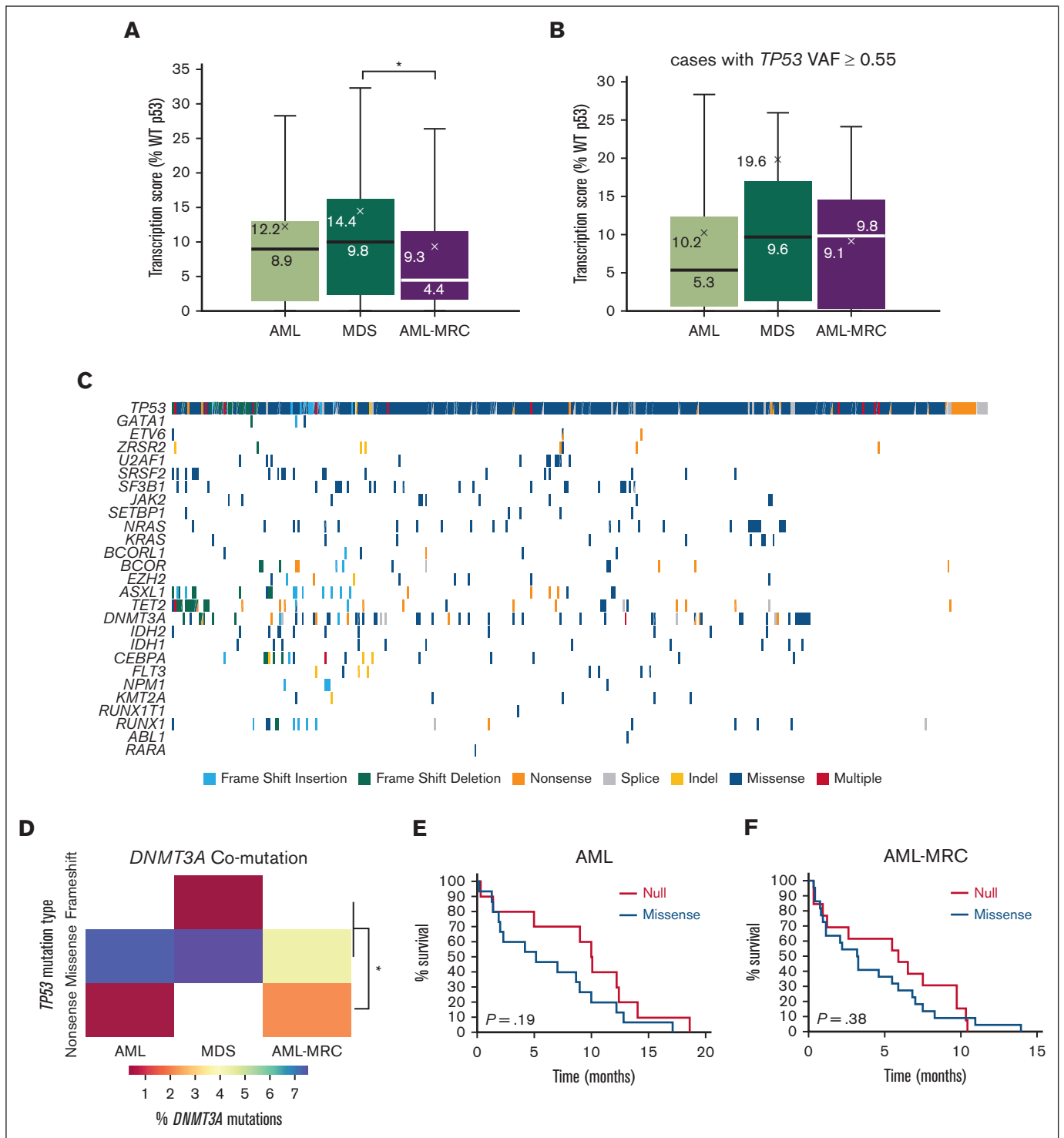


**Figure 4. p53 transcriptional activity and comutations vary between classes of neoplasia and *TP53* mutation types.** (A) Box and whisker plots of transcriptional activity scores of missense mutants in the indicated disease categories; AML,  $n = 408$ ; MDS,  $n = 282$ ; and AML-MRC,  $n = 113$ ;  $*P < .05$  by Welch  $t$  test with Bonferroni correction. (B) Box and whisker plots of transcriptional scores of missense mutants with VAF of  $\geq 0.55$  in the indicated neoplasms; AML,  $n = 79$ ; MDS,  $n = 32$ ; and AML-MRC,  $n = 30$ . In panels A-B, horizontal line indicates median, "X" marks the mean, and box top and bottom represent the 75th and 25th percentiles, respectively. Median (lower) and mean (upper) values are given for each bar. Error bars represent the 95% confidence interval. (C) Comutations in *TP53* with the indicated leukemic driver genes, segregated by *TP53* mutation type. (D) Comutations of *DNMT3A* with the indicated classes of *TP53* mutations in AML, MDS, or AML-MRC. Color indicates the percent of *DNMT3A* mutations cooccurring with the indicated class of *TP53* mutation.  $*P < .05$  by Fisher exact test comparing the association of *DNMT3A* mutation with the indicated *TP53* mutation type vs all other *TP53* mutation types. (E) Survival curves of AML ( $n = 10$  null, and  $n = 15$  missense *TP53*) or (F) AML-MRC ( $n = 13$  null, and  $n = 22$  missense *TP53*) patients with the indicated *TP53* mutation types. For panels E-F,  $P$  values calculated by Gehan-Breslow-Wilcoxon test.



fruitful in yielding both novel mechanistic insights and clinically useful correlations in solid tumors.<sup>40-42</sup> However, data derived from such sources are, by nature, heterogeneous in their analytical methods and clinical treatment protocols. Future studies using cohorts derived from single institutions will be critical to ensure that the conclusions are not influenced by hidden confounding variables that can occur in both overly homogeneous or heterogeneous data sets; furthermore, these studies may uncover additional associations or determine impacts of other variables (eg, blast count or monoallelic vs biallelic mutation) on the correlation between individual mutations/mutation classes and clinical outcomes.

We identified significant differences in *TP53* mutations between myeloid neoplasms and solid tumors. Most notably, we observed marked enrichment of mutations at codon Y220, which are relatively uncommon in solid tumors but were among the most frequent mutations in myeloid neoplasms in our data set. This finding is of particular interest because the properties of this mutant protein render it uniquely susceptible to reactivation by small-molecule stabilizers, particularly carbazole-based agents.<sup>43-45</sup> The p53-stabilizing agent eprentapopt has demonstrated efficacy in *TP53*-mutant myeloid neoplasms when used in combination with azacitidine and venetoclax.<sup>24-26</sup> Although this specific agent appears to have limited activity against Y220 mutants,<sup>46</sup> carbazoles are being evaluated in clinical trials for solid tumors.<sup>27,47</sup> Our findings thus argue for prioritizing evaluation of these agents in myeloid neoplasms. Furthermore, given that several p53-targeting agents currently in clinical trials have differential activity against specific mutations,<sup>48</sup> our findings illustrate the potential benefit of systematically identifying *TP53* mutations in myeloid neoplasms to identify patients who might benefit from this and other mutation-specific therapies.

Among myeloid neoplasms, MDS and AML-MRC showed the greatest differences in terms of their types, distributions, and predicted transcriptional activities of *TP53* mutations. These findings suggest that distinct types of *TP53* mutations mediate initiation of MDS and progression of MDS to AML. We find that R175H, G245S, and R282W were underrepresented in MDS and AML-MRC compared with AML; the R175H result is consistent with the study of Tashakori et al.<sup>20</sup> Conversely, R273H mutations were more common in MDS and AML-MRC than in AML. We found that missense mutations, particularly those retaining higher levels of transcriptional activity, are overrepresented in MDS, whereas mutations resulting in complete loss of expression or transcriptional activity of p53 protein are relatively overrepresented in AML-MRC. This result suggests that p53 missense mutations may play a more active role in initiation of MDS, possibly by acquiring gain-of-function properties, whereas p53 inactivation is sufficient for progression to AML-MRC. The specific association of *TP53* nonsense mutations with *DNMT3A* mutations in AML-MRC supports this hypothesis, because *DNMT3A* mutations (and, more broadly, mutations in genes that regulate chromatin accessibility and/or epigenetic control of gene expression) are common founder mutations in both MDS<sup>4</sup> and clonal hematopoiesis of indeterminate potential.<sup>49</sup> Notably, WT p53 protein can assume a “pseudomutant” conformation in hematopoietic stem cells, frequently in the presence of *DNMT3A* mutations, leading to mutant-like activation of downstream transcriptional pathways.<sup>50</sup> Thus, in this setting, *TP53* missense mutation may not provide additional selective

advantage to preleukemic clones, whereas truncating mutations may be capable of promoting further leukemogenesis and driving progression to AML-MRC. Overall, these findings raise the intriguing possibility that specific identification of *TP53* mutations in MDS may be useful in predicting which patients are likely to progress to AML. Tracking the evolution of *TP53* mutations in individual patients during progression from MDS to AML-MRC will be instrumental in further evaluation of this question. It would also be of interest to analyze the distribution of *TP53* mutations as a function of blast percentage in MDS, particularly in light of recent data indicating that the clinical impact of *TP53* mutation is different in MDS with and without excess blasts.<sup>17</sup> Although such analysis would require larger and more comprehensively annotated data sets than those used for this study, it might identify whether differences in the nature and distribution of mutations manifest at an even earlier stage than the transition from MDS to AML.

We observed that in both AML and AML-MRC, inactivating mutations tended to show longer survival than missense mutations, although these differences were not statistically significant. Prior studies demonstrating no significant survival difference between *TP53* mutation types did not distinguish between categories of myeloid neoplasia.<sup>20</sup> Our data suggest that more detailed multivariate analyses accounting for both neoplasm type and *TP53* mutation type will be required to conclusively determine the effects of *TP53* mutation class on patient survival. Notably, any differences in survival could arise from differences in *TP53* mutations themselves or from the spectrum of comutations, which varied according to neoplasm subtype as well as *TP53* mutation types. Specifically, *DNMT3A* mutations were associated with AML-MRC containing nonsense *TP53* mutations, but the consequences of this association remain unknown.

Clinical assessment of *TP53* mutation has historically operated under the guiding assumption that loss of functional p53 protein activity mediates its role in driving neoplasia, and, therefore, that specific identification and characterization of mutations are not clinically useful, and that p53 immunohistochemistry (a proxy for loss of protein function) is sufficient for diagnostic workup. This assumption is embedded in recent updates to classification schema for hematologic malignancies; both the fifth edition WHO classification and the ICC of myeloid neoplasms incorporate *TP53* mutation status into classification of myeloid malignancies,<sup>9,10</sup> but neither scheme incorporates mutation type or functional consequence. Our findings suggest that such assessment may be incomplete, and that assessment of *TP53* mutation type and consequences may be necessary to fully account for its impact on disease biology and prognosis.

## Acknowledgments

The authors thank Geoffrey Fell (Dana-Farber Cancer Institute), Derek Aguiar (University of Connecticut), Eliot Fenton (Harvard University), and Marie-Abele Bind (Massachusetts General Hospital) for help with statistical analysis; Jon Aster, Scott Rodig, and Annette Kim (Brigham and Women's Hospital) and Sandy Nandagopal and Meg Dillingham-McCullough (Harvard Medical School) for advice and critical review of the manuscript; and the members of the Brigham and Women's Hospital Department of Pathology and Harvard Medical School Department of Systems Biology for helpful discussion.

These studies were supported by funding from the Ludwig Institute at Harvard (A.J. and G.L.), the National Institutes of Health R35 GM139572 (G.L.), and the National Science Foundation Graduate Research Fellowship under grant no. DGE-2140743 (B.A.A.).

## Authorship

Contribution: A.J. and S.B.L. designed the concept, developed the study, and wrote the original draft of the manuscript; E.E.A. and B.A.A. performed computational and statistical analysis of data; G.L. advised the study and provided essential resources; and all authors contributed to the final version of the manuscript.

Conflict-of-interest disclosure: The authors declare no competing financial interests.

ORCID profiles: A.J., [0000-0003-1078-6601](#); E.E.A., [0000-0003-0735-7152](#); B.A.A., [0000-0002-1022-2163](#); G.L., [0000-0003-4758-6427](#); S.B.L., [0000-0001-9013-0105](#).

Correspondence: Ashwini Jambhekar, Department of Systems Biology, Harvard Medical School, 210 Longwood Ave, Armenise 605A, Boston, MA 02115; email: [ashwini\\_jambhekar@hms.harvard.edu](mailto:ashwini_jambhekar@hms.harvard.edu); and Scott B. Lovitch, Department of Pathology, Brigham and Women's Hospital, 75 Francis St, Amory 3, Boston, MA 02115; email: [slovitch@bwh.harvard.edu](mailto:slovitch@bwh.harvard.edu).

## References

1. Kasthuber ER, Lowe SW. Putting p53 in context. *Cell*. 2017;170(6):1062-1078.
2. Kandoth C, McLellan MD, Vandin F, et al. Mutational landscape and significance across 12 major cancer types. *Nature*. 2013;502(7471):333-339.
3. Cancer Genome Atlas Research N, Ley TJ, Miller C, et al. Genomic and epigenomic landscapes of adult de novo acute myeloid leukemia. *N Engl J Med*. 2013;368(22):2059-2074.
4. Papaemmanuil E, Gerstung M, Malcovati L, et al. Clinical and biological implications of driver mutations in myelodysplastic syndromes. *Blood*. 2013;122(22):3616-3627. quiz 3699.
5. Bejar R, Stevenson K, Abdel-Wahab O, et al. Clinical effect of point mutations in myelodysplastic syndromes. *N Engl J Med*. 2011;364(26):2496-2506.
6. Metzeler KH, Herold T, Rothenberg-Thurley M, et al. Spectrum and prognostic relevance of driver gene mutations in acute myeloid leukemia. *Blood*. 2016;128(5):686-698.
7. Rucker FG, Schlenk RF, Bullinger L, et al. TP53 alterations in acute myeloid leukemia with complex karyotype correlate with specific copy number alterations, monosomal karyotype, and dismal outcome. *Blood*. 2012;119(9):2114-2121.
8. Lindsley RC, Saber W, Mar BG, et al. Prognostic mutations in myelodysplastic syndrome after stem-cell transplantation. *N Engl J Med*. 2017;376(6):536-547.
9. Khoury JD, Solary E, Abal O, et al. The 5th edition of the World Health Organization classification of haematolymphoid tumours: myeloid and histiocytic/dendritic neoplasms. *Leukemia*. 2022;36(7):1703-1719.
10. Arber DA, Orazi A, Hasserjian RP, et al. International Consensus Classification of myeloid neoplasms and acute leukemias: integrating morphologic, clinical, and genomic data. *Blood*. 2022;140(11):1200-1228.
11. Grob T, Al Hinai ASA, Sanders MA, et al. Molecular characterization of mutant TP53 acute myeloid leukemia and high-risk myelodysplastic syndrome. *Blood*. 2022;139(15):2347-2354.
12. Weinberg OK, Siddon A, Madanat YF, et al. TP53 mutation defines a unique subgroup within complex karyotype de novo and therapy-related MDS/AML. *Blood Adv*. 2022;6(9):2847-2853.
13. Sallman DA, Komrokji R, Vaupel C, et al. Impact of TP53 mutation variant allele frequency on phenotype and outcomes in myelodysplastic syndromes. *Leukemia*. 2016;30(3):666-673.
14. Bernard E, Nannya Y, Hasserjian RP, et al. Implications of TP53 allelic state for genome stability, clinical presentation and outcomes in myelodysplastic syndromes. *Nat Med*. 2020;26(10):1549-1556.
15. Ball S, Singh AM, Ali NA, et al. A product of "Clash of Titans" or true reflection of disease biology? Validation of 2022 WHO and ICC classifications in a large dataset of patients with myelodysplastic syndrome. *Blood*. 2022;140(suppl 1):1118-1120.
16. Stengel A, Haeflrich T, Baer C, et al. Specific subtype distribution with impact on prognosis of TP53 single-hit and double-hit events in AML and MDS. *Blood Adv*. 2023;7(13):2952-2956.
17. Stengel A, Meggendorfer M, Walter W, et al. Interplay of TP53 allelic state, blast count, and complex karyotype on survival of patients with AML and MDS. *Blood Adv*. 2023;7(18):5540-5548.
18. Leroy B, Anderson M, Soussi T. TP53 mutations in human cancer: database reassessment and prospects for the next decade. *Hum Mutat*. 2014;35(6):672-688.
19. Kato S, Han SY, Liu W, et al. Understanding the function-structure and function-mutation relationships of p53 tumor suppressor protein by high-resolution missense mutation analysis. *Proc Natl Acad Sci U S A*. 2003;100(14):8424-8429.
20. Tashakori M, Kadia T, Loghavi S, et al. TP53 copy number and protein expression inform mutation status across risk categories in acute myeloid leukemia. *Blood*. 2022;140(1):58-72.
21. Cluzeau T, Loschi M, Fenaux P, Komrokji R, Sallman DA. Personalized medicine for TP53 mutated myelodysplastic syndromes and acute myeloid leukemia. *Int J Mol Sci*. 2021;22(18):10105.

22. Daver NG, Maiti A, Kadia TM, et al. TP53-mutated myelodysplastic syndrome and acute myeloid leukemia: biology, current therapy, and future directions. *Cancer Discov.* 2022;12(11):2516-2529.
23. Sallman DA, McLemore AF, Aldrich AL, et al. TP53 mutations in myelodysplastic syndromes and secondary AML confer an immunosuppressive phenotype. *Blood.* 2020;136(24):2812-2823.
24. Cluzeau T, Sebert M, Rahme R, et al. Eprenetapopt plus azacitidine in TP53-mutated myelodysplastic syndromes and acute myeloid leukemia: a phase II Study by the Groupe Francophone des Myelodysplasies (GFM). *J Clin Oncol.* 2021;39(14):1575-1583.
25. Garcia-Manero G, Goldberg AD, Winer ES, et al. Eprenetapopt combined with venetoclax and azacitidine in TP53-mutated acute myeloid leukaemia: a phase 1, dose-finding and expansion study. *Lancet Haematol.* 2023;10(4):e272-e283.
26. Sallman DA, DeZern AE, Garcia-Manero G, et al. Eprenetapopt (APR-246) and azacitidine in TP53-mutant myelodysplastic syndromes. *J Clin Oncol.* 2021;39(14):1584-1594.
27. Dumbrava EE, Johnson ML, Tolcher AW, et al. First-in-human study of PC14586, a small molecule structural corrector of Y220C mutant p53, in patients with advanced solid tumors harboring a TP53 Y220C mutation. *J Clin Oncol.* 2022;40(suppl 16):3003.
28. Cerami E, Gao J, Dogrusoz U, et al. The cBio cancer genomics portal: an open platform for exploring multidimensional cancer genomics data. *Cancer Discov.* 2012;2(5):401-404.
29. Gao J, Aksoy BA, Dogrusoz U, et al. Integrative analysis of complex cancer genomics and clinical profiles using the cBioPortal. *Sci Signal.* 2013;6(269):pl1.
30. Tyner JW, Tognon CE, Bottomly D, et al. Functional genomic landscape of acute myeloid leukaemia. *Nature.* 2018;562(7728):526-531.
31. Yoshida K, Sanada M, Shiraishi Y, et al. Frequent pathway mutations of splicing machinery in myelodysplasia. *Nature.* 2011;478(7367):64-69.
32. Papaemmanuil E, Gerstung M, Bullinger L, et al. Genomic classification and prognosis in acute myeloid leukemia. *N Engl J Med.* 2016;374(23):2209-2221.
33. Welch JS, Petti AA, Miller CA, et al. TP53 and decitabine in acute myeloid leukemia and myelodysplastic syndromes. *N Engl J Med.* 2016;375(21):2023-2036.
34. Bouaoun L, Sonkin D, Ardin M, et al. TP53 variations in human cancers: new lessons from the IARC TP53 Database and Genomics Data. *Hum Mutat.* 2016;37(9):865-876.
35. Olivier M, Hollstein M, Hainaut P. TP53 mutations in human cancers: origins, consequences, and clinical use. *Cold Spring Harb Perspect Biol.* 2010;2(1):a001008.
36. Vaddavalli PL, Schumacher B. The p53 network: cellular and systemic DNA damage responses in cancer and aging. *Trends Genet.* 2022;38(6):598-612.
37. de Andrade KC, Lee EE, Tookmanian EM, et al. The TP53 Database: transition from the International Agency for Research on Cancer to the US National Cancer Institute. *Cell Death Differ.* 2022;29(5):1071-1073.
38. Kadia TM, Jain P, Ravandi F, et al. TP53 mutations in newly diagnosed acute myeloid leukemia: clinicomolecular characteristics, response to therapy, and outcomes. *Cancer.* 2016;122(22):3484-3491.
39. Hou HA, Chou WC, Kuo YY, et al. TP53 mutations in de novo acute myeloid leukemia patients: longitudinal follow-ups show the mutation is stable during disease evolution. *Blood Cancer J.* 2015;5(7):e331.
40. Jiao XD, Qin BD, You P, Cai J, Zang YS. The prognostic value of TP53 and its correlation with EGFR mutation in advanced non-small cell lung cancer, an analysis based on cBioPortal data base. *Lung Cancer.* 2018;123:70-75.
41. Hou H, Zhang C, Qi X, et al. Distinctive targetable genotypes of younger patients with lung adenocarcinoma: a cBioPortal for cancer genomics data base analysis. *Cancer Biol Ther.* 2020;21(1):26-33.
42. Brlek P, Kafka A, Bukovac A, Pecina-Slaus N. Integrative cBioPortal analysis revealed molecular mechanisms that regulate EGFR-PI3K-AKT-mTOR pathway in diffuse gliomas of the brain. *Cancers (Basel).* 2021;13(13):3247.
43. Bauer MR, Kramer A, Settanni G, et al. Targeting cavity-creating p53 cancer mutations with small-molecule stabilizers: the Y220X paradigm. *ACS Chem Biol.* 2020;15(3):657-668.
44. Bauer MR, Jones RN, Tareque RK, et al. A structure-guided molecular chaperone approach for restoring the transcriptional activity of the p53 cancer mutant Y220C. *Future Med Chem.* 2019;11(19):2491-2504.
45. Basse N, Kaar JL, Settanni G, Joerger AC, Rutherford TJ, Fersht AR. Toward the rational design of p53-stabilizing drugs: probing the surface of the oncogenic Y220C mutant. *Chem Biol.* 2010;17(1):46-56.
46. Liu X, Wilcken R, Joerger AC, et al. Small molecule induced reactivation of mutant p53 in cancer cells. *Nucleic Acids Res.* 2013;41(12):6034-6044.
47. Hassin O, Oren M. Drugging p53 in cancer: one protein, many targets. *Nat Rev Drug Discov.* 2023;22(2):127-144.
48. Nishikawa S, Iwakuma T. Drugs targeting p53 mutations with FDA approval and in clinical trials. *Cancers (Basel).* 2023;15(2):429.
49. Jaiswal S, Fontanillas P, Flannick J, et al. Age-related clonal hematopoiesis associated with adverse outcomes. *N Engl J Med.* 2014;371(26):2488-2498.
50. Tuval A, Brilon Y, Azogy H, et al. Pseudo-mutant P53 is a unique phenotype of DNMT3A-mutated pre-leukemia. *Haematologica.* 2022;107(11):2548-2561.